Disposable Microfluidic Channel with Dielectric Layer on PCB for AC Sensing of Biological Cells

Jinhong Guo
Singapore University of Technology and Design
Pillar of Engineering Product Development
Singapore 138682, Singapore

Yuejun Kang
Nanyang Technological University
School of Chemical and Biomedical Engineering
62 Nanyang Drive, Singapore 637459, Singapore

and **Ye Ai**
Singapore University of Technology and Design
Pillar of Engineering Product Development
Singapore 138682, Singapore

ABSTRACT

In this paper, we report a disposable microfluidic impedance cytometer attached on a reusable printed circuit board (PCB) with dielectric layer for single cell detection. The cover slide acts as a dielectric layer which allows the AC signal to sense the impedance change cross the microfluidic channel. The microfluidic chip can be disposed; while the bottom PCB with pre-deposited electrodes is reusable after each sample test. We experimentally demonstrate that the developed device is able to selectively detect HeLa cells, a type of umor cells, and ignore Red Blood Cells (RBCs). Integration of low cost and disposable microfluidic chip with reusable PCBs widely available in the industry is of great potential in point of care diagnosis of cancer, especially in the developing countries.

Index Terms - **Disposable device, microfluidics, impedance Cytometer, dielectric layer, PCB , RBCs.**

1 INTRODUCTION

VARIOUS strategies have been implemented in recent years for the detection and enumeration of CTCs, such as electrochemical detection [1], immunomagnetic detection [2], and fluorescence detection [3] etc. However, most of these methods require tedious and time-consuming sample pre-processing for the immunoassay or use of expensive fluorescent labels. Some of these detection methods even need to be supported by expensive and bulky optical detection systems. For example, the commercial flow cytometer is the most widely used platform for clinical diagnostics of hematological disorders. However, the cost per test is very high and thus limits its application in the developing countries or resource-limited regions. As a low cost diagnostic platform, impedance based microfluidic

Cytometry has been widely applied for the detection of pollen [4], biological cells [5, 6, 7], bacteria [8], viruses [9], DNA and other biomolecules [10,11,12]. The working principal of impedance cytometry is based on the mechanism when a single particle carried by electrolytes translocates through a micro/nano-scale pore, the electrical impedance of the pore can significantly increase due to the physical blockage by the particle, accordingly leading to a significant change in the electrical current through the pore. Microfluidic impedance cytometry is preferable due to its significant reduction of cost as compared to the conventional optical flow cytometry.

However, many reported microfluidic impedance cytometry devices require precise patterning of electrodes on a silicon or glass substrate, followed by a well-aligned bonding of a microchannel onto this functionalized substrat [13, 14] Obviously it is a non-trivial task to pattern tiny electrodes on silicon or glass substrate, which requires complicated surface processing to achieve the desired strong bonding between the metallic layer and the substrate material [15, 16]. This approach still requires considerable

Manuscript received on 7 September 2014, in final form 20 January 2014, accepted 26 January 2015.

DOI 10.1109/TDEI.2015.004917

cost for the device fabrication and therefore limits its wide application for point of care diagnosis. To address this problem, we develop a microfluidic impedance cytometer combined with reusable electrodes on a PCB, as the concept indicated in Figure 1. Biological sample is loaded in a microfluidic chip made of a polymer material and a glass cover slide. The disposable microfluidic chip is placed on the top of a PCB for test and can be disposed after test. As the electrodes on the PCB are not in physical contact with biological samples, the PCB is reusable for future tests. Hence, the microfluidic impedance cytometer could provide a highly cost-effective platform for point of care diagnosis.

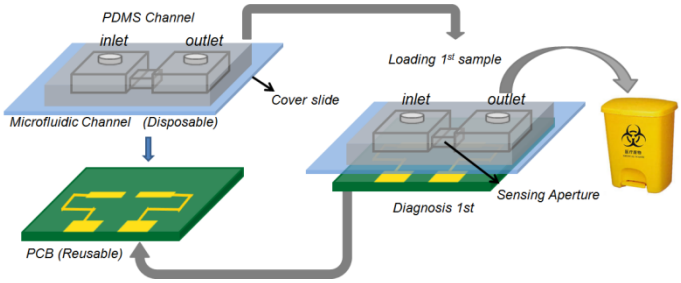

Figure 1. The Schematic illustration of the microfluidic impedance cytometer. A microfluidic channel bonded onto a glass cover slide is disposable; while electrodes on a PCB are reusable. After each test, a new microfluidic chip will be attached on the PCB for the subsequent test.

2 Theory and Method

This section covers the details regarding preparation of your manuscript for submission, the submission procedure, review process and copyright information. Figure 2a illustrates a simplified equivalent circuit model of the impedance cytometry when a microfluidic channel is placed above the electrodes on a PCB. The electrolyte in the microfluidic channel can be modeled as a resistor. The parasitic capacitance Ce between the two electrodes is considered in the circuit model [17-18]. The glass cover slide as the microfluidic substrate between the electrolytes and electrodes is modeled as a capacitor with a capacitance of Cs, which also includes the capacitance of electrical double layer at the substrate/liquid interface [19]. Consequently, by applying an AC voltage signal with angular frequency ω, the input impedance without a microparticle in the sensing aperture can be written as:

$$Z_{in} = \frac{1}{j\omega C_e} \cdot \frac{j\omega + \frac{2}{RC_s}}{j\omega + \frac{1}{R}\left(\frac{1}{C_e} + \frac{2}{C_s}\right)} \tag{1}$$

When a single microparticle or biological cell moves through the sensing aperture, the change in impedance appears due to the presence of less-conductive particle instead of the conductive electrolytes, which in turn induces a decrease in the measured electrical current. The current change with respect to the impedance change can be derived as [17]:

$$\frac{\Delta I}{\Delta R} \approx \frac{dI}{dR} = \frac{dI}{dZ}\cdot\frac{dZ}{dR} = -\frac{1}{R^2}\cdot\left(\frac{j\omega}{j\omega + \frac{2}{RC_s}}\right)^2 \cdot V_{in} \tag{2}$$

Consequently, the change in the current amplitude can be simplified as:

$$|\Delta I| \approx \frac{\Delta R}{R^2}\cdot\left(\frac{\omega^2}{\omega^2 + (\frac{2}{RC_s})^2}\right)\cdot V_{in} \tag{3}$$

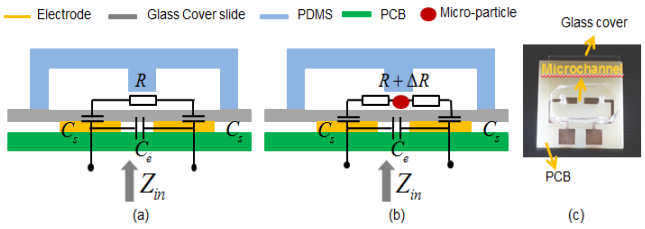

Figure 2. (a) Equivalent circuit model of the impedance cytometer without a microparticle/cell in the sensing aperture. R is the resistance of the electrolytes in the aperture, Ce is the parasitic capacitance between two electrodes, Cs is the equivalent capacitance between electrode and carrying electrolytes (b) Impedance modulation by a transient blockage of a microparticle/cell (c) Photograph of the device.

The impedance modulation induced by a spherical particle through the sensing aperture is related to the particle size, as derived by Gregg and Steidley [20]:

$$\Delta R \approx -\frac{\rho V_p}{\pi^2 r_m^4}\left(\frac{1 + 0.3K^2 + 0.13K^4}{\sqrt{1-K^2}}\right) \tag{4}$$

where Vp is the particle volume and K is the diameter ratio between the particle and the aperture. ρ is the fluid resistivity. Therefore, the particle size can be detected with the evaluation of the impedance modulation by measuring the change in the output current amplitude. In the measurement, system noise plays a destructive role in the output signal evaluation, which means the signal induced by small particles may be buried in the noise. Fortunately, enumeration of tumor cell is only interested in the detection of tumor cell in blood samples. As long as the device can sense the impedance modulation by tumor cell, although the signal induced by blood cells is buried in the noise, the device is still meaningful in clinical applications. The device performance in distinguishing tumor cell from RBCs is discussed in details in the experimental part.

The simulation is performed by a commercial Finite Element Method package COMSOL Multiphysics 4.3b (COMSOL, CA, USA). The COMSOL AC/DC module can compute the electrical field by solving the following equation:

$$E = -\nabla V \tag{5}$$

where V is the electrical potential, E is the electrical field strength. The electric current density can be written as:

$$J = \sigma E + j\omega D \tag{6}$$

where J is the current density, σ is the electrical conductivity, D is the electrical displacement field, ω is the angular frequency.

The boundary conditions at the electrodes are given by

Excitation electrode: V=1 V (7a)

Grounded electrode: V=0 V (7b)

The particle surface and the outer wall are assumed non-conducting:

$$\vec{n} \cdot \nabla V = 0 \tag{8}$$

An adaptive mesh set was applied to the model. In the sensing aperture region, ultra-fine mesh was used with maximum mesh size of 0.5 μm, and minimum mesh size of 0.1 μm. For the rest of the computation domain, fine mesh was employed with maximum mesh size of 10 μm and minimum mesh size of 1 μm. The AC voltage excitation has a magnitude of 1 V and frequency sweep range is from 200 KHz to 800 KHz. As shown in Fig. 3, the model is composed of four components. The dimension of microfluidic channel is 300 μm in width and 60 μm in height. The aperture dimension is 20 μm × 20 μm × 20 μm. The thickness of the glass cover is 150 μm. The simulation parameters are summarized in Table 1.

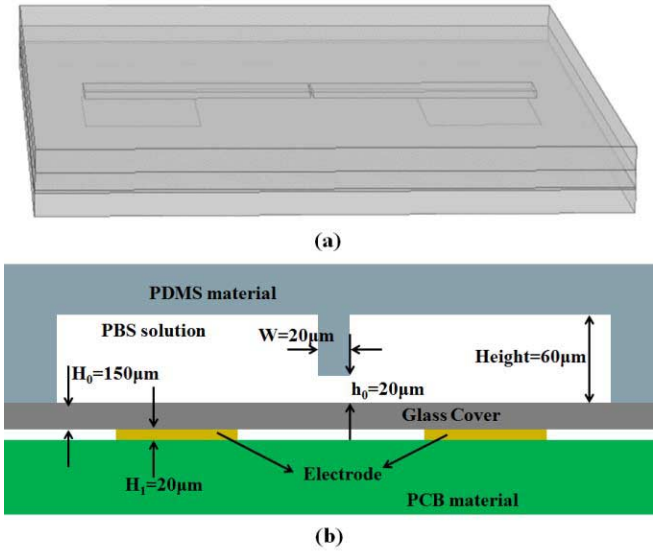

Figure 3. (a) Schematic view of the 3-D model; (b) Cross-sectional view of the device geometry in the simulation.

Table S1. Major parameters used in *the* simulation.

	Dielectric Constant	Electrical Conductivity
PDMS	2.55	$1x10^{-12}$ s/m
PBS solution	80	1.6 s/m
PCB	4	$1x10^{-12}$ s/m
Glass cover	4.7	$1x10^{-14}$ s/m

3 Device Fabrication and Experiment Setup

A mold of the polydimethylsiloxane (PDMS) microfluidic channel was fabricated by patterning two layers of photoresist (SU-8 25, Microchem, MA, USA) on a glass slide5, which was cleaned in acetone, methanol, and de-ionized water, and dried on a hot plate at 250°C for 30 min. PDMS pre-polymer and curing agents were mixed at a weight ratio of 10:1, and then degassed in a vacuum chamber. The mixture was poured on the SU-8 mold and baked in an oven at 95 °C for 2 hours. PDMS channels were then sliced and peeled off from the SU-8 mold and reservoir holes were punched. The PDMS channel and a clean cover slide were surface-activated using plasma for 10s before they were bonded to form the final chip, as shown in Figure 2c. The fabricated sensing aperture in the microfluidic channel is 20 μm in width, 20 μm in high, and 20 μm in length. The PCB with a pair of pre-deposited electrodes (2 mm apart) was obtained from a commercial supplier (HQPCB, Shen Zhen, China) at a unit price less than US$1.00. High vacuum grease was applied at the bottom of the microfluidic chip in order to guarantee a stable and sealed contact with the electrodes on the PCB. A mechanical pump (PHD 22/2000, Harvard Apparatus) was applied to drive continuous flowing samples into the device. The two electrodes on the PCB were connected to a function generator and a lock-in amplifier (SR850, Stanford Research Instruments, USA). The current change due to the physical blockage of biological cells was monitored by the input impedance of the lock-in amplifier, which converts the current signal to a voltage signal. The output voltage signal was sampled with the data acquisition card and data capture software (LabVIEW, National Instruments, USA) for post processing.

In order to demonstrate the selective detection of biological cells, both HeLa cell (average diameter of 16 μm) and human RBCs (average equivalent diameter of 5 μm) were prepared for device test. The RBCs were collected from the bottom of the centrifuge tube after centrifugation of a whole blood sample at 2000 gav for 15 min. Subsequently, the RBCs were re-suspended in PBS. HeLa cells (American Type Culture Collection, MD, USA), a typical type of HeLa cells, were cultured in a T75 flask containing the Dulbecco's Modified Eagle Medium (DMEM) supplement with 10% fetal bovines serum (FBS), 1mM sodium pyruvae, 0.1 mM MEM nonessential amino acids at 37 0C under 5% CO2.

4 RESULT AND DISCUSSION

A numerical simulation is performed by a commercial Finite Element Method package COMSOL Multiphysics 4.3b (COMSOL, CA, USA) to investigate the effect of applied signal frequency on the electrical current through the sensing aperture. Figure 4 indicates the current density flow at four different frequencies: 200, 400, 600 and 800 kHz (Details of the numerical model are provided in the supporting information). At a higher frequency of the input AC voltage, the current density through the aperture is stronger since a higher frequency signal is easier to penetrate the glass cover substrate as compared to a lower frequency signal.

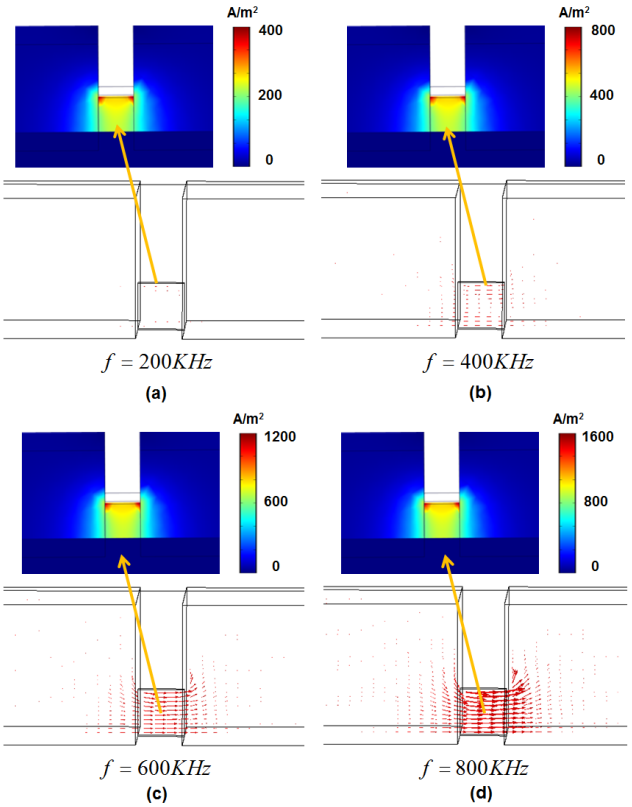

Figure 4. Current density through the sensing aperture at 200 kHz (a), 400 kHz (b), 600 kHz (c) and 800 kHz (d) signal excitation.

Figure 5a illustrates the impedance modulation induced by the translocation of individual polystyrene particles with 15.23 µm in diameter through the sensing aperture recorded at 200, 400, 600 and 800 kHz, respectively. The measurements indicate that no peak was captured at the frequency 200KHz. Based upon Equ.3, at a lower frequency, the factor $\omega^2 / \left(\omega^2 + (2/RC_s)^2\right)$ is relatively small so that the signal was buried in the system noise. For other frequencies above 200 kHz, the increase in the impedance signal becomes measurable for single particle detection. When polystyrene particles with 6.55 µm in diameter passed through the sensing aperture, no peak was detected at all the four frequencies, 200, 400, 600, and 800 kHz, as shown in Figure 5b. Equation (4) reveals that the resistance change is proportional to the particle size that is a cubic function of the particle diameter. Therefore, ΔR induced by the 6.55 µm particle was relatively small and thus buried in the system noise.

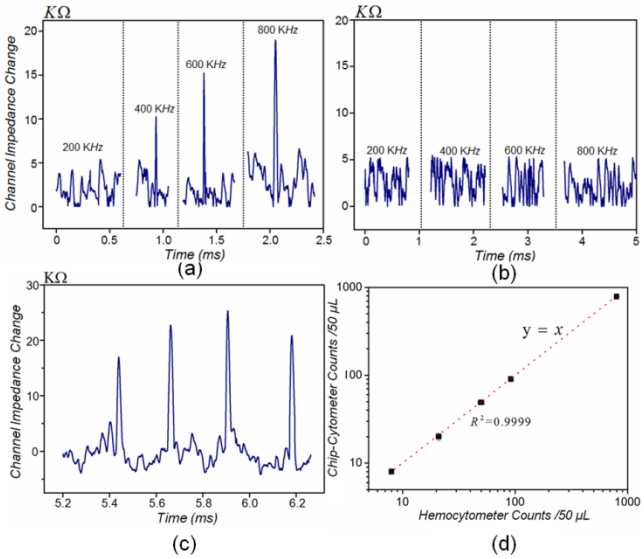

Figure 5. (a) Typical impedance modulation obtained by monitoring the current amplitude at frequency 200KHz, 400KHz, 600KHz, 800KHz when 15.23 µm polystyrene particles translocate through the sensing aperture. The signal is buried in the noise at 200KHz and becomes measureable at other higher frequencies. (b) Impedance modulation induced by 6.55 µm polystyrene particles. No measurable impedance change was detected at all the four frequencies. (c) Measured impedance change in amplitude at 800 KHz due to the translocation of four HeLa Cells through the sensing aperture. (d) Comparison of HeLa cell enumeration by the developed device and Hemocytometer with known concentrations.

We also used RBCs and HeLa cells samples to test and validate the developed device for selective cell detection. The measurement of RBCs indicates that no significant peak of output signal was found. This observation is attributed to the relatively small size of RBCs as compared to the sensing aperture. As a result, the impedance change due to the translocation of RBCs was covered by the noise. For HeLa cells enumeration, HeLa cells at specific concentrations were measured using both the microfluidic impedance cytometer and a commercial Hemocytometer. Figure 5c shows a series of typical spikes of impedance change with operating frequency at 800 kHz to demonstrate the detection and enumeration of HeLa cells using the developed device. Each spike corresponds to the translocation of one single HeLa cell. Fig. 5d further compares the HeLa cells enumeration performed by our device and a commercial Hemocytometer, which shows that our microfluidic impedance cytometer has a good accuracy as compared to the commercial cytometer. In summary, the signal induced by RBCs is covered by noise; while the signal induced by HeLa cells can be detected by the device. Therefore, the disposable microfluidic cytometer has great potential to provide reliable detection and enumeration of tumor cells in blood samples, which is a promising low cost technique for point of care diagnosis, especially in the developing world.

7 CONCLUSION

We have reported a cost effective microfluidic impedance cytometer built upon a reusable PCB with pre-deposited electrodes that is widely available in industry with unit price less than $2. Diagnosis can be continuously performed by replacing new disposable microfluidic channels on the PCB. The presented device successfully demonstrated its capability in the detection and enumeration of HeLa cells for low cost diagnosis. In the future work, we will further integrate the post-processing circuit system to build a compact measurement system for the test of whole blood samples from cancer patients.

ACKNOWLEDGMENT

This research is supported by a seed grant from Sustainable Earth Office at Nanyang Technological University and Tier-1 Academic Research Fund from Singapore Ministry of Education (RG 26/11) awarded to Y.K. and SUTD-MIT International Design Center IDG11300101 awarded to Y.A.

REFERENCES

[1] T. S. Pui, P. Kongsuphol, S. K. Arya and T. Bansal, "Detection of tumor necrosis factor (TNF-α) in cell culture medium with label free electrochemical impedance spectroscopy", Sensors and Actuators B, Vol. 181, pp. 494-500, 2013.

[2] K. Hoshino, Y. Y. Huang, N. Lane, M. Huebschman, J. W. Uhr, E. P. Frenkel and X. Zhang, "Microchip-based immunomagnetic detection of circulating tumor cells", Lab Chip, Vol. 11, pp. 3449-3457, 2011.

[3] X. L. Li, S. Shan, M. Xiong, X. H. Xia, J. J. Xu and H.Y. Chen, "On-chip Selective Capture of Cancer Cells and Ultrasensitive Fluorescence Detection of Survivin mRNA in single Living Cells", Lab Chip, Vol. 13, pp. 3868 -3875, 2013.

[4] Z. Zhang, J. Zhe, S. Chandra and J. Hu, "An electronic pollen detection method using Coulter counting principle", *Atmospheric Environment*, Vol. 39, No. 30, pp. 5446-5453, 2005.

[5] J. Mehdi and H. T. AmirAli, "Target cell detection based on microchannel gating", Biomicrofluidics, Vol. 1, pp. 044103, 2007.

[6] S.-Y. Teh, R. Khnouf, H. Fan and A.P. Lee, "Stable, biocompatible lipid vesicle generation by solvent exraction-based droplet microfluidics", Biomicrofluidics, vol. 5, pp. 44113, 2011.

[7] A. C. Sabuncu, J. Zhuang, J. F. Kolb and A. Beskok, "Microfluidic impedance spectroscopy as a tool for quantitative biology and biotechnoogy", Biomicrofluidics, vol. 6, pp. 034103, 2012.

[8] H. E. Kubitschek, and J. A. Friske, "Determination of bacterial cell volume with the Coulter Counter", J. Bacteriol, Vol. 168, No. 3, pp. 1466-1477, 1986.

[9] G. Damhorst, B. M. Venkatesan, S. Banerjee, V. Solovyeva and R. Bashir, "A submicron Coulter Counter for enumeration of viruses and nanoparticels", Biophys J., Vol. 102, No. 3, pp. 584a, 2012.

[10] J. S. Lorenz, O. Oliver, C. Catalin, G. Joanne and F. K. Ulrich, "Detecting DNS folding with nanocapillaries", Nano Letter., Vol. 10, No. 7, pp. 2493-2497, 2010.

[11] H. Bayley, C. R. Martin, "Single-cell microfluidic impedance cytometry: a review", Chem Rev, Vol. 100, No. 7, pp. 2575-2594 , 2000.

[12] C. Dekker, "Solid-state nanopores", Nat. Nano, Vol. 2, No. 4, pp. 209-215, 2007.

[13] K.C. Cheung, M. D. Berardino, G. Schade-Kampmann, M. Hebeisen, A. Pierzchalski, J. Bocsi, A. Mittag, and A. Tarnok, "Microfluidic impedance-based flow cytometry", Cytometry Part A, Vol. 77, No. 7, pp. 648-666, 2010.

[14] T. Sun and H. Morgan,"Single-cell microfluidic impedance cytometery: a review", Microfluid Nanofluid, Vol. 8, No. 4, pp. 423-443, 2010.

[15] H. Song, Y. Wang, J. M. Rosano, B. Prabhakarpandian, C. Garson, K. Pant and E. Lai, "A microfluidic impedance cytometer for identification for differentiation state of stem cells", Lab Chip, Vol. 13, No. 12, pp. 2300-2310, 2013.

[16] M. Evander, A. J. Ricco, J. Morser, G. T. A. Kovacs, L. L. K. Leung and L. Giovangrandi, "Microfluidic impedance cytometer for platelet analysis", Lab Chip, Vol. 13, No. 4, pp. 722-729, 2013.

[17] S. Emaminejad, M. Javanmard, R. W. Dutton and R. W. Davis, "Microfluidic diagnostic tool for the developing world: contactless impedance flow cytometry", Lab Chip, Vol. 12, No. 21, pp. 4499-4507, 2012.

[18] J. Guo, C.M and Li, Y. Kang, "PDMS-film coated on PCB for AC Impedance Sensing of Biological Cells", Biomedical Microdevices, Vol. 16, No. 5, pp. 681-686, 2014.

[19] A. Venkatanarayanan, T. E. Keyes and R. J. Forster, "Rare cell separation and analysis by magnetic sorting", Anal Chem, Vol. 85, No. 4, pp. 2216-2222, 2013.

[20] E. C. Gregg and K. D. Steidley,"Electrical counting and sizing of mammalian cells in suspension", Biophys J., Vol. 5, No. 4, 393-405, 1965.

Jinhong Guo (M'14) received his B.E. in electronic engineering in 2010 from the University of Electronic Science and Technology of China (UESTC) and the Ph.D. degree in 2014 in biomedical engineering from Nanyang Technological University (NTU). He worked as Research Engineer for RFIC design at VIRTUS Integrated Circuit Design Lab in NTU from 2011 to 2011. In 2011- 2014, he worked as a research assistant at Applied Microfluidicological Lab jointly with Institute of Microelectronics, A*STAR, Singapore. Since April 2014, he co-founded the JESON Technology co. , ltd and is now appointed as the Chief Scientist. Dr. Jinhong published many patents, which have been commercialized by JESON. He has first/co-author more than 20 journals and international conference papers. His research interests include Micro/Nano Solid-State Biosensor, Electrofluidics, Acoustofluidics, Optofluidics Sensor and Actuator, Nano-Electromagnetics, Microwave Cytometry. He also serves the reviewer of many journals such as, *IEEE Transactions, Lab On a Chip, Biomicrofluidics, Biomedical Microdevice, Microfluidics and Nanofluidics, Electrophoresis, Progress In Electromagnetic Research etc.*

Yuejun Kang earned his Ph.D. degrees in mechanical engineering from Vanderbilt University in 2008 and Nanyang Technological University (NTU) in 2005, respectively. Before he joined the School of Chemical Biomedical Engineering at NTU as an assistant professor in 2011, Yuejun worked as a postdoctoral researcher in Monash University and Los Alamos National Laboratory. His current research is focused on micro/nano-fluidics based bio-instrumentation using electrical, optical, acoustical, and biochemical methods for analysis of biological cells/elements with biomedical, bio-energy, and environmental applications.

Ye Ai obtained his B.S. degree in mechanical engineering from Huazhong University of Science and Technology (China) in 2005, and his Ph.D. degree in mechanical and aerospace engineering from Old Dominion University (USA) in 2011. From 2005 to 2008, he worked as a research associate at Wuhan National Laboratory for Optoelectronics (China). Prior to joining SUTD as an assistant professor, he worked as a postdoctoral researcher and expanded his research in bioengineering at Los Alamos National Laboratory (USA). Dr Ai's professional expertise lies on Micro/nanofluidics, BioMEMS and Lab-on-a-chip. His research aims to develop low cost and field-deployable devices for various biomedical, energy and environmental applications.